Table 1. Cerebrovascular lesions, the time and findings of/from diagnostic imaging, and treatment in each patient

Patient No.	Age	Sex	Site of cerebrovascular lesion	Infarct No.	Site of infarct	From onset to MRI[1]	From MRI to SPECT[2]	Treatment
1	23	F	Moyamoya disease, bilateral ICA stenosis (+) (bil. stage IIIc)	1	Lt. MCA perfusion territory	18	4	Bilateral EDAS (77 days) Aspirin therapy
2	68	M	Lt. ICA stenosis (95%), Rt. ICA stenosis (70%)	2a	Lt. MCA perfusion territory	7	4	Urokinase therapy (0 days)
				2b	Lt. occipital pole	Unknown		Heparin → warfarin therapy
				2c	Rt. external capsule	Unknown		Lt. carotid endarterectomy (102 days)
				2d	Rt. putamen	Unknown		
				2e	Lt. middle temporal gyrus	Unknow		
3	72	F	Rt. ICA occlusion, Lt. ICA stenosis (75%)	3a	Rt. mid-brain	1	3	Anticoagulation therapy → warfarin therapy
				3b	Rt. basal ganglia	1		
4	4	M	Moyamoya disease (bil. stage IIIb)	4	Lt. anterolateral angle	1	0	Bil. EDAS (8 days)
5	1	F	Moyamoya disease, bilateral ICA occlusion (+)	5a	Lt. PCA perfusion territory	1	0	Warfarin therapy
				5b	Rt. MCA perfusion territory	24		(post-bil. EDAS)
6	79	M	Lt. PCA stenosis	6a	Lt. thalamus	1	5	Urokinase therapy (0 days)
				6b	Rt. putamen	Unknown		Antiplatelet therapy
				6c	Lt. putamen	Unknown		
7	12	F	Moyamoya disease, bilateral ICA stenosis (+) (Rt. stage II, Lt. stage II–IIIa)	7a	Lt. middle frontal gyrus	8	2	Aspirin therapy
				7b	Rt. superior frontal gyrus	44		Rt. EDAS (60 days)
8	52	M		8	Lt. posterior parietal artery	2	7	Aspirin therapy
9	61	F	Lt. M1 occlusion, Rt. IC aneurysm	9	Lt. middle temporal gyrus	581	2	
10	52	F	Lt. MCA occlusion	10	Lt. semoval center	74	0	
11	45	F	Moyamoya disease (Lt. EDAS) Lt. MCA occlusion, Rt. ACA occlusion Rt. MCA stenosis	11	Lt. middle temporal gyrus	984	0	

[1] Days from the episode of stroke symptom which caused the infarct to initial MRI in this study.
[2] Days from initial MRI to SPECT.

Is it correct to say that the size of an infarct is determined during the acute stage in most cases, and that it does not change thereafter? It is known that some infarcts show a tendency towards extension even after the acute stage [2]. To our knowledge, however, no report has been published concerning the long-term changes in the sizes of infarcts during the subacute to chronic stages.

The present study was undertaken to examine the long-term changes in the sizes of infarcts, the relationship between the sizes of infarcts and the extent of the surrounding hypoperfused areas, and the background of such changes.

Patients, Materials and Methods

Of all the patients who underwent MRI at the Department of Radiology of our hospital for detailed evaluation following the occurrence of cerebral ischemic stroke between January 1998 and May 2001, those who had infarcts and underwent cerebral angiography were selected for this study. Eleven patients (4 males and 7 females, age range 1–72 years, mean age 42.6 years) with a total of 20 foci of infarcts were registered for this study (table 1). All these 11 patients underwent brain SPECT (^{99m}Tc-ethyl cysteinate dimer) within 1 week after initial MRI, and underwent MRI again more than half a year later. The following patients were excluded from the evaluation: 1 patient who developed another focus of infarct in the vicinity of the first one during the follow-up period, and 4 patients with small infarcts ($\leq$10 mm) in the deep white matter that could not be detected by SPECT.

For each patient, the cerebral angiogram images obtained after the attack were analyzed to check for underlying cerebrovascular lesions. Of the 11 patients, 7 were found to have severe stenotic lesions of the internal carotid arteries bilaterally. Of the remaining 4 patients, 2 had MCA occlusion, 1 had stenosis of the PCA, and 1 had no cerebrovascular lesions.

MR Imaging

In the present study, MRI was used for the detection of infarcts. MR images were obtained using a 1.5-Tesla system (Magnetom Vision, Siemens Medical Systems, Erlangen, Germany; Signa, General Electric Medical Systems, Milwaukee, Wisc., USA). The size of the infarct was determined from transverse T_2-weighted MR images (repetition time 4,000 ms; echo time 96.2 ms; matrix size 256 × 256; field of view 200 mm; section thickness of 4 mm with an intersection gap of 0.4 mm).

SPECT Scanning

SPECT was used to detect hypoperfused tissue around the infarct core, using ^{99m}Tc-ethyl cysteinate dimer as the tracer; 800 MBq of the tracer was injected into the right cubital vein of the patient lying in the supine position.

Fifteen minutes after the injection, SPECT imaging was performed using a triple-head rotating gamma camera Prism 3000 (Picker International, Cleveland, Ohio, USA) equipped with low-energy, ultra-high-resolution fan beam collimators. The resulting data were processed using Odyssey software. Images were obtained under the following conditions: 140 keV energy, 15% window, 4-degree steps, 90 directions, 30 s per direction, and a 128 × 128 matrix. The spatial resolution of the scanner was 3.8 mm full-width-at-half-maximum (FWHM). The entire imaging process required about 20 min to perform. All SPECT data were reconstructed using a three-dimensional post-filter (Butterworth) with a cut-off frequency of 0.24 cycles/pixel and an order of 4.0. Chang's method was used to correct the data for absorption (Chang, 0.09/cm). Transverse images, with a slice thickness of 1.72 mm, were obtained parallel to the OM line.

SPM

One disadvantage of SPECT images is that the sizes or sites of hypoperfused areas are not clearly represented, making their comparison with other images difficult. To overcome this disadvantage, we used the statistical parametric mapping (SPM) software (SPM 96 for Windows, Wellcome Department of Cognitive Neurology, London, UK). We conducted the Jackknife test with a normal database for many people, and projected statistically significantly hypoperfused areas onto the standardized brain. In this way, it was possible to objectively represent the sites and sizes of hypoperfused areas.

Data from 36 normal volunteers (10 males and 26 females, age range 20–67 years, mean age 44.4 years) were used as the normal database. These healthy volunteers were free of neurological or psychiatric illness (including alcoholism, drug addiction, atypical headaches, head trauma with disturbed consciousness, and asymptomatic cerebral infarction detectable on T_2-weighted MR images). Informed consent was obtained from all the healthy volunteers. The study was approved by the Ethics Committee of our university.

Each SPECT image was spatially normalized to the stereotaxic space of the Montreal Neurological Institute brain, in order to remove inter-individual morphological differences. The spatial normalization included both affine transformations and a linear combination of smooth spatial basis functions (7 × 8 × 7 mm) for modeling global nonlinear differences in shape. The spatially normalized structural images were resliced to a final voxel size of approximately 2 × 2 × 2 mm^3.

After conversion, the images were smoothed with a 12-mm FWHM Gaussian filter to increase the signal/noise ratio. To examine regional differences, the images were scaled to a mean global cerebral blood flow of 50 ml/100 g/min.

The differences in relative rCBF per voxel were tested by the t-test. The t value was subjected to z conversion so that the mean and standard deviation would become 0 and 1 in the normal distribution, respectively. In this way, areas showing statistically significant differences ($p = 0.001$) were identified. Bonferroni correction ($p = 0.05$) was also performed, considering multiple comparisons. Based on the results of these analyses, changes in the cerebral blood flow following ischemia were projected onto the axial images of the standard brain.

Image Analysis

MRI and SPM studies were evaluated with blinded separate interpretations by two independent radiologists. When the observers did not fully agree, diagnosis was achieved by consensus. The radiologists were blinded to clinical information, such as patient's presenting symptoms.

Lesions in the deep white matter with less blood flow than the cortex are difficult to detect by brain perfusion scintigraphy. That is, scintigraphy is not suitable for evaluation of the progression of cortical infarction towards deeper white matter. In the present study, we compared only the anteroposterior lengths of the infarcts and did not compare the widths, which mainly corresponds to the progress of the infarct in the direction of the deep white matter.

Using SPM, the anteroposterior lengths of significantly hypoperfused areas ($p < 0.001$) were measured, and their percentages relative to the anteroposterior lengths of the cerebral hemisphere (hypoperfusion brain ratio; HBR %) were calculated (fig. 1A).

Also on T_2-weighted MR images, the anteroposterior diameters of hyperintense lesions were measured manually, and their percentages relative to the anteroposterior length of the cerebral hemisphere (infarct brain ratio; IBR %) were calculated (fig. 1B). To exclude the influence of hypoperfused areas appearing anew after the performance of the SPECT, we measured the anteroposterior lengths of only the areas showing scar-like changes and not the surrounding, slightly high-signal intensity areas that did not show signs of scarring, when measuring the anteroposterior lengths of hyperintense lesions on MR images taken more than 1 year after the onset of stroke.

For each infarct, the number of days, which had elapsed after the episode of stroke symptom, was also recorded (table 1). The number of elapsed days was estimated not only for infarcts that were directly responsible for the stroke, and necessitated the MRI and SPECT study, but also for infarcts, which caused previous stroke detected on MR images simultaneously. For the six old infarcts detected in 2 patients, the dates of onset could not be identified, because these patients had not visited our clinic before the onset of the stroke.

Results

When comparing the HBR and IBR within 1 week, no subject had an IBR/HBR ratio between 39 and 75%; therefore, the subjects were divided into a group with a

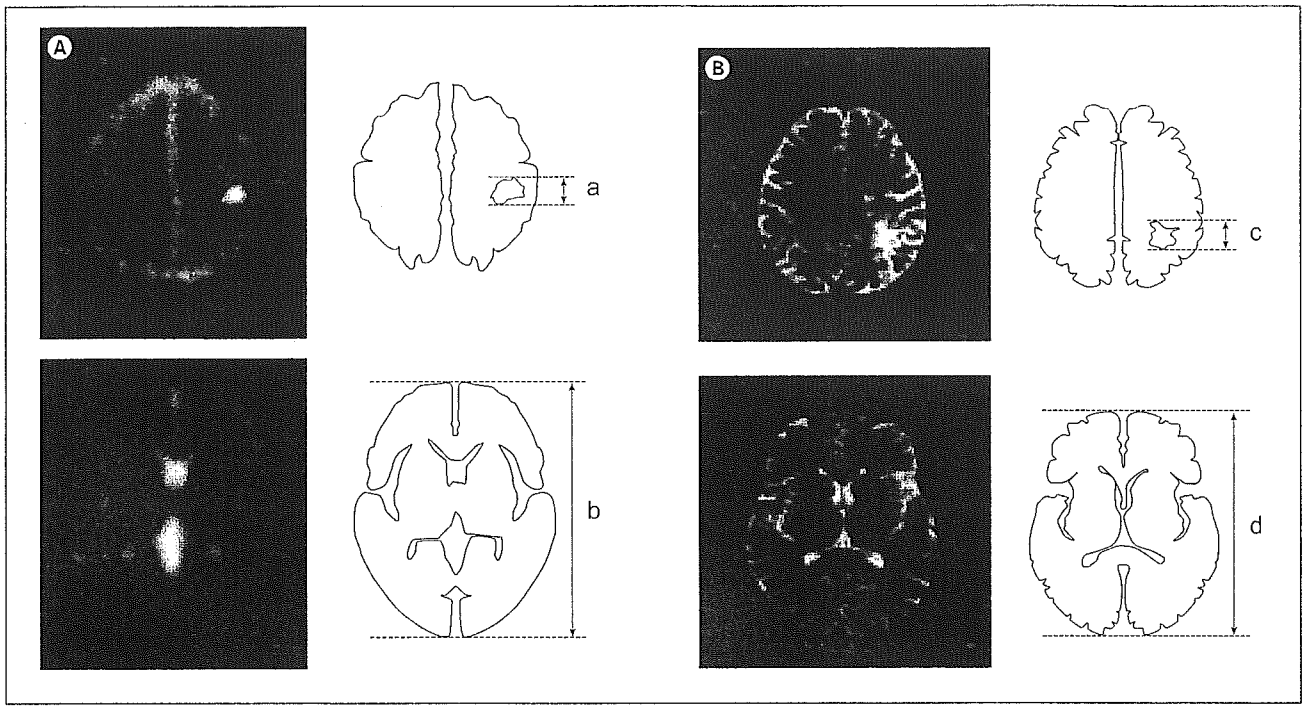

1

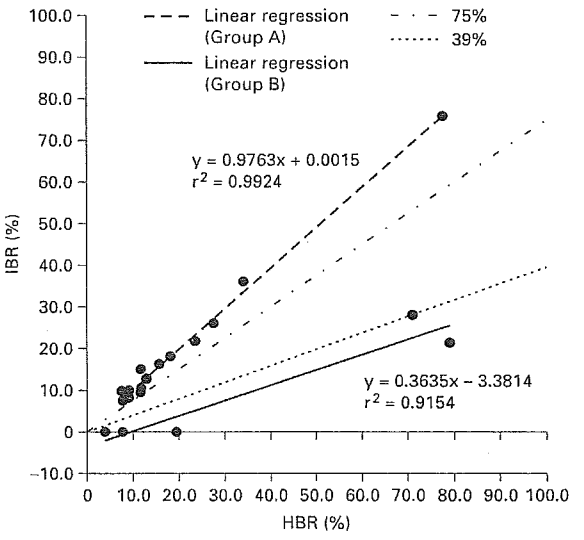

2

Fig. 1. Projection of a significantly hypoperfused area ($p < 0.001$) detected by SPECT onto the standard brain using SPM (**A**). The percentage of the anteroposterior length of the SPM significantly hypoperfused area relative to the anteroposterior length of the cerebral hemisphere (hypoperfusion brain ratio; HBR %) was calculated. Also on T_2-weighted MR images (**B**), the percentage of the anteroposterior length of the hyperintense lesion relative to the anteroposterior length of the cerebral hemisphere (infarct brain ratio; IBR %) was calculated. **A** HBR = a/b × 100(%). **B** IBR = c/d × 100(%).

Fig. 2. Comparison of the HBR with IBR on MRI and SPECT images taken at around the same time. The patients were divided into two groups: group A with a IBR/HBR ratio of over 75% and group B with a ratio below 40%. In group A, the linear regression was defined by Y = 0.976X +0.002 and the multiple correlation coefficient (R^2) was 0.992. In group B, linear regression was defined by Y = 0.364X +3.338 and R^2 was 0.915.

large IBR/HBR ratio (75–125%) and a group with a small IBR/HBR ratio (0–39%), as shown in figure 2. Nine patients (15 lesions) were assigned to group A (large IBR/HBR ratio group), and 5 patients (5 lesions) were allocated to group B (small IBR/HBR ratio group). In group A, a very high correlation was noted between the infarct size and extent of significant hypoperfusion.

When the time-course of changes was followed, infarcts in group A showed little change in size (fig. 3, 5). In group B, all infarcts increased slowly, and after more than

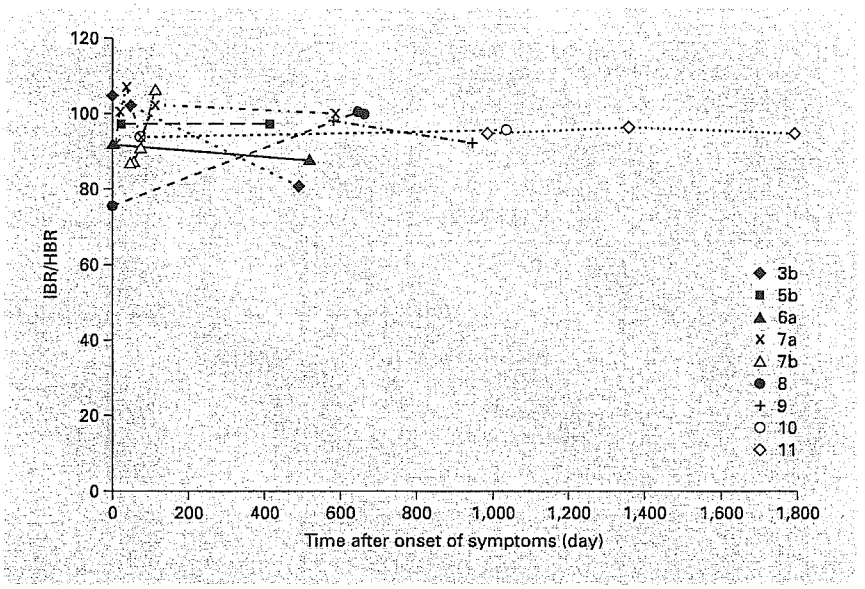

Fig. 3. Time-course of changes in the anteroposterior length of the infarct on T_2-weighted MR images in group A. The Y axis indicates the percentage relative to the surrounding hypoperfused area (IBR/HBR). No significant change in the size of the infarct was noted.

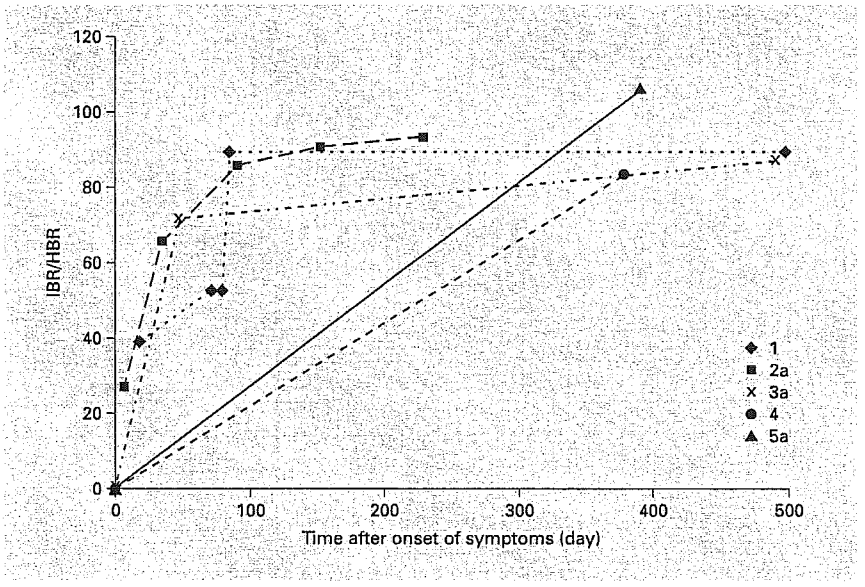

Fig. 4. Time-course of changes in the anteroposterior length of infarcts on T_2-weighted MR images in group A. Each infarct showed a significant tendency of growth. All the infarcts followed for short periods of time showed slow enlargement.

half a year, each IBR/HBR ratio of group B increased to the ratio of group A (75–125%) (fig. 4, 6).

When the relationship between infarction and cerebrovascular disease was analyzed, all patients with infarcts in group B had severe stenosis of the internal carotid arteries bilaterally (table 2). Conversely, of all 7 patients with severe stenosis of the internal carotid arteries of both sides, 5 patients had infarcts in group B. All 4 patients without internal carotid artery lesion had only infarcts assigned to group A.

Table 2. Relationship between bilateral internal carotid artery stenosis and size of infarction in group B

	Group B (+)[1] (n = 5)	Group B (–)[2] (n = 6)
Bilateral ICA stenosis (+) (n = 7)	5	2
ICA stenosis (–) (n = 4)	0	4

[1] Patients with infarcts in group B.
[2] Patients without infarcts in group B.

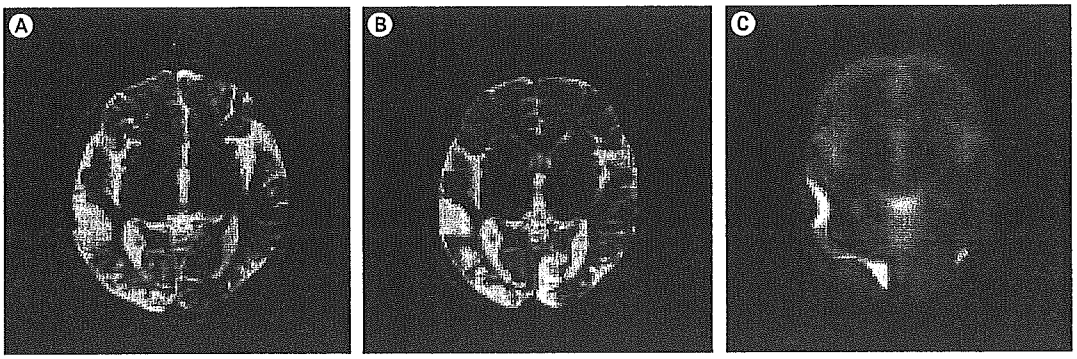

Fig. 5. One-year-old girl with moyamoya disease (group A). Admitted for detailed examination and treatment. On the day following EDAS, the patient developed left-sided hemiplegia. SPECT conducted 23 days after the onset revealed a broad hypoperfused area in the right MCA through the PCA region (**C**). Partially hypoperfused areas were also seen in the left watershed region. T_2-weighted MRI, conducted 24 days after onset, disclosed an infarct approximately identical with the hypoperfused area (**A**). T_2-weighted MRI on the 414th day showed no marked change in the infarct size in the said region (**B**). The new infarct seen in the left PCA region seems to have developed during the follow-up period.

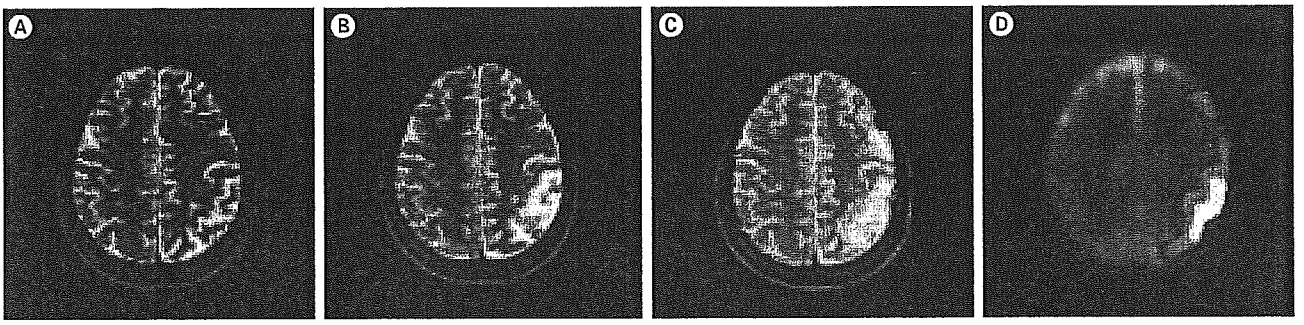

Fig. 6. A 23-year-old woman with moyamoya disease (group B). Admitted after development of hemiplegia on the right side. T_2-weighted MRI conducted 18 days after the onset revealed a slightly high-intensity area around the left angular gyrus (**A**). SPECT conducted on the 22nd day showed a surrounding hypoperfused area with an anteroposterior length three times that of the said region (**D**). MRI on the 72nd day revealed a tendency towards enlargement (**B**). The final infarct (on the 498th day) was approximately identical with the significantly hypoperfused area visible on the initial SPM (**C**). On the 77th day, the patient was treated surgically by bilateral EDAS.

The relationship between the slow enlargement of the infarcts and the clinical symptoms cannot be represented as a numerical value because of the retrospective nature of this study. However, the clinical records of 4 of the 5 patients with infarcts in group B showed that a clinical exacerbation of symptoms (thought to be caused by the infarct) was observed during the period when the infarcts were increasing in size. Since the 1 remaining patient had a PCA territory infarct and aphasia, a clear exacerbation of her symptoms was not seen.

Discussion

In cases of acute ischemic stroke, the infarcted core is usually surrounded by hypoperfused tissue. This abnormally perfused area is considered to be 'tissue at risk', and is called 'ischemic penumbra', if the abnormality is reversible [5, 12, 13]. In the present study, the size of the infarct in many cases was equal to the size of the area showing significant hypoperfusion on the first MR images, while some infarcts were much smaller than the

hypoperfused area. What does the presence of such a broad hypoperfused area around an infarct imply?

In the present study, broad hypoperfusion was seen in 5 cases. In all of these 5 cases, severe stenosis or occlusion of the internal carotid arteries was noted bilaterally. Neumann-Haefelin et al. [14] also reported that the size of the perfusion-weighted image (PWI)/diffusion-weighted image (DWI) mismatch was much greater in patients with severe lesions of the internal carotid artery than in patients not showing carotid artery stenosis. In these cases, collateral flow probably develops as a result of persistence of severe internal carotid artery lesions. It seems therefore likely that even when thromboembolism has taken place, collateral flow, mainly via the circle of Willis, partially compensates for the local follow obstruction at the site of stenosis. Among other possible factors, it seems likely that thrombi in cases of carotid artery stenosis are smaller than those in patients with a cardiac source of the emboli, causing less severe ischemia.

The sizes of the infarcts did not change with time in the group in which the infarct size was the same as the surrounding area showing significant hypoperfusion. On the other hand, in the group of patients showing broader hypoperfused areas, the rate to the hypoperfused area of infarct increased, and after more than half a year, turned into the same rate as the former group. All of the infarcts followed up for short periods of time showed only slow growth, taking more than a month to grow to a size of about 75% of the size of the surrounding hypoperfused area.

Regarding the growth of infarcts, it is often said that the size reaches a peak within 1 week, more significantly during the first 3 days after the onset of stroke [1]. It is also known that some infarcts continue to grow thereafter [2].

In the study conducted by Du et al. [15] using rats, infarction due to severe ischemia (lasting for 90 min) was completed within a day, while infarction due to moderate ischemia (lasting for 30 min) took about 2 weeks to grow to a size equivalent to the peak size of the infarct caused by severe ischemia. In the latter case, apoptosis rather than ordinary necrosis may contribute to the growth of the infarct [2, 15]. In the present study, all patients showing a slow growth of the infarct had severe stenosis of the internal carotid artery bilaterally. It is highly possible that in these patients, continued moderate ischemia, instead of severe ischemia caused by embolism, etc., was operative. The involvement of apoptosis is also possible in these cases.

However, the very slow growth of infarcts observed in this study cannot be fully explained by these factors alone. It seems possible that in addition to continuous mild ischemia around the infarct, other factors may be involved in delayed infarct enlargement, including: (a) possible repetition of embolism at the stenosed site, (b) reduction in the cerebral circulatory reserve, and (c) effects of antiplatelet or anticoagulation therapy administered soon after the onset of stroke.

In the present study, all infarcts surrounded by broad areas of hypoperfusion grew for more than half a year to a size equal to the size of the initial hypoperfused area. This suggests that the hypoperfused tissue around an infarct, as detected on SPM, does not eventually survive, even though much time is taken until this area loses all viability. Are there any therapeutic means that can prevent the enlargement of infarcts?

It has been suggested that more infarcts in the penumbra region can be prevented by intra-arterial fibrinolytic therapy than by standard heparin therapy [16]. In the present study, many patients had undergone urokinase therapy in the very acute stage of the disease. However, since pretreatment SPECT images for these patients were unavailable, we could not evaluate the effects of this therapy.

All of our patients received antiplatelet or anticoagulation therapy in the acute stage of the disease. Of the 5 patients in whom the infarcts showed a tendency towards further growth, 3 were treated surgically. We could not confirm in any case whether or not surgical or medical treatment could prevent the progression of infarction to the hypoperfused area.

Some investigators reported that the volume of the penumbra, which did not advance into infarction in the acute stage, was closely related to subsequent neurological recovery [6, 17]. This suggests that neuronal reorganization may take place in the noninfarcted surrounding area. However, the present study suggests that in many cases, the infarction advances to the hypoperfused areas after a relatively long period of time; simultaneous with the infarct's extension, the clinical exacerbation of symptoms thought to be caused by the infarct is often seen. The relationship between this slow enlargement of the infarcts and the course of neurological findings needs further study.

This study has several limitations. First, the age distribution of the patients was broader than that of the normal SPM database, and especially child data was not contained in the contrast group. However, it was morally impossible to have created a child's normal database.

Second, in this study the sizes of the infarcts and the hypoperfused areas were measured as the anteroposterior length, which is not necessarily related to changes in the

volume. For example, it is possible that persistence of infarction can result in scar-like changes, associated with a decrease in volume due to slit-shaped contraction. This change is not reflected in the anteroposterior length.

Third, the present study was a retrospective study, and SPECT images were obtained at varying points of time after the onset of stroke (in the acute stage in some cases and in the subacute stage in others). Furthermore, follow-up SPECT images were not available for the patients. For these reasons, the time-course of changes in the sizes of the hypoperfused areas could not be followed. Moreover, the intervals between the initial MRI and SPECT assessments ranged from the same day to 7 days apart, so the SPECT imaging results did not necessarily depict the early stage of the perfusion abnormality.

In conclusion, many of the patients with severe bilateral lesions of the carotid artery had broad hypoperfused areas around the infarcts. The infarction progressed to these hypoperfused areas after long periods of time. These results indicate that patients with stenosis of the internal carotid artery often have slowly growing infarcts, and that SPM is useful for predicting the ultimate size of the infarcts.

References

1 Lansberg MG, O'Brien MW, Tong DC, Moseley ME, Albers GW: Evolution of cerebral infarct volume assessed by diffusion-weighted magnetic resonance imaging. Arch Neurol 2001;58:613–617.

2 Pantano P, Caramia F, Bozzao L, Dieler C, von Kummer R: Delayed increase in infarct volume after cerebral ischemia: Correlations with thrombolytic treatment and clinical outcome. Stroke 1999;30:502–507.

3 Schwamm LH, Koroshetz WJ, Sorensen AG, Wang B, Copen WA, Budzik R, Rordorf G, Buonanno FS, Schaefer PW, Gonzalez RG: Time course of lesion development in patients with acute stroke: Serial diffusion- and hemodynamic-weighted magnetic resonance imaging. Stroke 1998;29:2268–2276.

4 Wittsack HJ, Ritzl A, Fink GR, Wenserski F, Siebler M, Seitz RJ, Modder U, Freund HJ: MR imaging in acute stroke: Diffusion-weighted and perfusion imaging parameters for predicting infarct size. Radiology 2002;222: 397–403.

5 Karonen JO, Nuutinen J, Kuikka JT, Vanninen EJ, Vanninen RL, Partanen PL, Vainio PA, Roivainen R, Sivenius J, Aronen HJ: Combined SPECT and diffusion-weighted MRI as a predictor of infarct growth in acute ischemic stroke. J Nucl Med 2000;41:788–794.

6 Furlan M, Marchal G, Viader F, Derlon JM, Baron JC: Spontaneous neurological recovery after stroke and the fate of the ischemic penumbra. Ann Neurol 1996;40:216–226.

7 Watanabe Y, Takagi H, Aoki S, Sassa H: Prediction of cerebral infarct sizes by cerebral blood flow SPECT performed in the early acute stage. Ann Nucl Med 1999;13:205–210.

8 Ueda T, Yuh WT, Maley JE, Quets JP, Hahn PY, Magnotta VA: Outcome of acute ischemic lesions evaluated by diffusion and perfusion MR imaging. AJNR Am J Neuroradiol 1999; 20:983–989.

9 Baird AE, Austin MC, McKay WJ, Donnan GA: Sensitivity and specificity of ^{99m}Tc-HMPAO SPECT cerebral perfusion measurements during the first 48 h for the localization of cerebral infarction. Stroke 1997;28:976–980.

10 Barber PA, Darby DG, Desmond PM, Yang Q, Gerraty RP, Jolley D, Donnan GA, Tress BM, Davis SM: Prediction of stroke outcome with echoplanar perfusion- and diffusion-weighted MRI. Neurology 1998;51:418–426.

11 Hirano T, Read SJ, Abbott DF, Barid AE, Yasaka M, Infeld B, Barber PA, Davis SM, McKay WJ, Donnan GA: Prediction of the final infarct volume within 6 h of stroke using single photon emission computed tomography with technetium-99m hexamethylpropylene amine oxime. Cerebrovasc Dis 2001;11:119–127.

12 Neumann-Haefelin T, Wittsack HJ, Wenserski F, Siebler M, Seitz RJ, Modder U, Freund HJ: Diffusion- and perfusion-weighted MRI. The DWI/PWI mismatch region in acute stroke. Stroke 1999;30:1591–1597.

13 Hossmann KA: Viability thresholds and the penumbra of focal ischemia. Ann Neurol 1994; 36:557–565.

14 Neumann-Haefelin T, Wittsack HJ, Fink GR, Wenserski F, Li TQ, Seitz RJ, Siebler M, Modder U, Freund HJ: Diffusion- and perfusion-weighted MRI: Influence of severe carotid artery stenosis on the DWI/PWI mismatch in acute stroke. Stroke 2000;31:1311–1317.

15 Du C, Hu R, Csernansky CA, Hsu CY, Choi DW: Very delayed infarction after mild focal cerebral ischemia: A role for apoptosis. J Cereb Blood Flow Metab 1996;16:195–201.

16 Klotz E, Konig M: Perfusion measurements of the brain: Using dynamic CT for the quantitative assessment of cerebral ischemia in acute stroke. Eur J Radiol 1999;30:170–184.

17 Mounts JM, Modell JG, Foster NL, DuPree ES, Ackermann RJ, Petry NA, Bluemlein LE, Kuhl DE: Prognostication of recovery following stroke using the comparison of CT and technetium-99m HM-PAO SPECT. J Nucl Med 1990;31:61–66.

ELSEVIER

Neuroscience Letters 339 (2003) 123–126

Neuroscience Letters

www.elsevier.com/locate/neulet

Fronto-parieto-cerebellar interaction associated with intermanual transfer of monkey tool-use learning

Shigeru Obayashi[a,b,*], Tetsuya Suhara[a], Koichi Kawabe[a], Takashi Okauchi[a], Jun Maeda[a], Yuji Nagai[a], Atsushi Iriki[b]

[a]*Brain Imaging Project, National Institute of Radiological Sciences, CREST (JST), Chiba 263-8555, Japan*
[b]*Section of Cognitive Neurobiology, Department of Maxillofacial Biology, Tokyo Medical and Dental University, Tokyo 113-8549, Japan*

Received 27 September 2002; received in revised form 13 December 2002; accepted 18 December 2002

Abstract

Prior motor skill learning (original learning; OL) with one hand (original hand; OH) can affect relearning of the same skill (transfer learning; TL) with the opposite hand (transferred hand; TH). This phenomenon is known as intermanual transfer of learning. We explored specialization of brain activation underlying tool-use between hands by measuring regional cerebral blood flow in two monkeys using positron emission tomography. We found brain activation specified for TL in the bilateral prefrontal cortex, bilateral intraparietal sulcus region, and cerebellum contralateral to TH. The results suggest that those regions may be related to intermanual transfer of tool-use learning, presumably in terms of modifying a motor engram specific for OH.

Keywords: Prefrontal cortex; Intraparietal sulcus; Cerebellum; Positron emission tomography; Procedural memory; Transfer of learning; Japanese macaque

The phenomenon of appropriately transferring knowledge and skills acquired in one setting to another is known as the transfer of learning. We observed intermanual transfer when monkeys learned to obtain a distant reward using a rake-shaped tool. It took about 2 weeks to complete original hand (OH) learning (original learning; OL), whereas with the opposite hand (transferred hand; TH) it took only a few days to relearn the same task (transferred learning; TL).

We recently demonstrated that OL produced remarkable changes in the cortex around the intraparietal sulcus (IPS). The changes led to cortical reorganization such as significant increases in expression of brain-derived neurotrophic factor, its receptor trkB, and neurotrophin-3 [5]. Simultaneously, neurons in the IPS area became sensitive to visual stimuli [3]. However, as TL was completed within a few days, such plastic cortical changes would be unlikely to occur. We hypothesized that the hemisphere underlying tool-use by TH (TH activation) may not simply be symmetrical to OH activation.

Firstly, we aimed to find the difference in learning curves between OL and TL. Secondly, to test our hypothesis, we obtained TH activation for comparison with OH activation, which was based on an earlier study showing right-hand tool-use-related activities by positron emission tomography (PET) with $H_2^{15}O$ [12]. OH activation showed increased activities in higher motor cortices, the IPS region contralateral to OH, bilateral inferotemporal cortices (IT), bilateral basal ganglia, and bilateral cerebellum. In the present study, regional cerebral blood flow (rCBF) during tool-use task with TH was measured in two monkeys by the same method as the earlier study.

Three awake Japanese monkeys (*Macaca fuscata*, males, 4–5 kg; M_{1-3}) were used. M_1 and M_2 underwent PET scans. M_3 was used only for behavioral analysis. OH was right for M_1 and M_3, meaning that the transfer direction was right-to-left. OH was left for M_2.

The monkeys were implanted with a plastic headset device attached to the skull with acrylic screws and dental cement. This plastic device can be used for head-fixation to a chair and is compatible with MRI. All surgery was performed with sodium pentobarbital (Nembutal at 30 mg/kg, i.v.) and aseptic techniques.

M_1 and M_2 were the same animals as in the earlier study (corresponding to monkeys A and B, respectively) [12]. OH

* Corresponding author. Tel.: +81-43-206-3249; fax: +81-43-206-0396.
E-mail address: ohbayash@nirs.go.jp (S. Obayashi).

0304-3940/03/$ - see front matter © 2003 Elsevier Science Ireland Ltd. All rights reserved.
doi:10.1016/S0304-3940(02)01477-5

training was extended for one (M_2) or 2 months (M_1) after OL completion. The interval between OL and TL was about 6 months. TH training was continued for 2 months.

Duration of training for each hand and inter-training interval of M_3 were 2 weeks, respectively. Each trial required a response to a visual cue, a food pellet (Precision Food Pellets; P.J. NOYES Co., Inc., Lancaster, NH) with a rake. Trials were aborted for an error in the situation of the rake no longer able to access the pellet, or for a 'time-out' (no response to the pellet within 30 s). Following a total of 200 trials of daily training, 30 trials were done to obtain the learning curve. Behavior during training was captured by video camera (CCD-PC1; Sony, Tokyo, Japan) from above. Captured images entered a video timer (time resolution 100 ms; VTG-55; FOR.A Inc., Tokyo, Japan), and videotaping was done by digital videocassette recorder (SVO-5800; Sony, Tokyo, Japan). The learning curves of OL and TL were estimated by success rate (SR), reaction time (RT), and movement time (MT). SR consisted of successful trials of the monkey finally obtaining the pellet directly despite many misses. Trials without misses were termed SRF (SR at first contact). RT was the response time between placing the pellet and grasping the rake. MT was the time of the rake action to the moment of catching the pellet with the rake.

Behavioral results are illustrated in Fig. 1. Learning curves of OL reached a plateau after 14 days, whereas those of TL took only a few days. Of note is that there was no response to the target for 9 days in OL. M_3 could not respond to the target until discovering an abstract strategy for handling the rake. In contrast, M_3 was active from the first day of TH, meaning that M_3 already knew what to do with the rake. RT and MT for OL reached a plateau in performance within 5 days of the response to a reward, whereas those for TL reached a plateau within 2 days. Thus, we speculate that what was transferred between OL and TL was not simply an abstract strategy but something to facilitate a product of the motor act for TH, namely a "motor engram", a kind of motor imagery on guidance of tool-use.

Monkeys were fixed upright to the chair and scanned during the following two tasks [12]. In the tool-use task, they had to retrieve an out-of-reach pellet with a rake-shaped tool with TH. The pellets were presented by dispenser onto the table in random order (Fig. 2a–1). Thirty trials were performed for every PET scan. In the simple-stick-manipulating task as the control task, the monkeys had to manipulate a simple-stick (identical to the shaft of the tool) in their preferred directions with TH before the pellet was presented within reach (Fig. 2a–2). Thirty trials were performed for every PET scan.

A PET camera (SHR-7700; Hamamatsu Photonics Inc., Hamamatsu, Japan) was used in enhanced 2D mode (31 slices; 111.6 mm axial field of view; 2.6 mm spatial resolution). Thirty-one images (3.6 mm slice thickness) were acquired simultaneously, covering the whole monkey brain. After a 30 mCi bolus $H_2^{15}O$-tracer injection, scanning was started when rising brain radioactivity was first

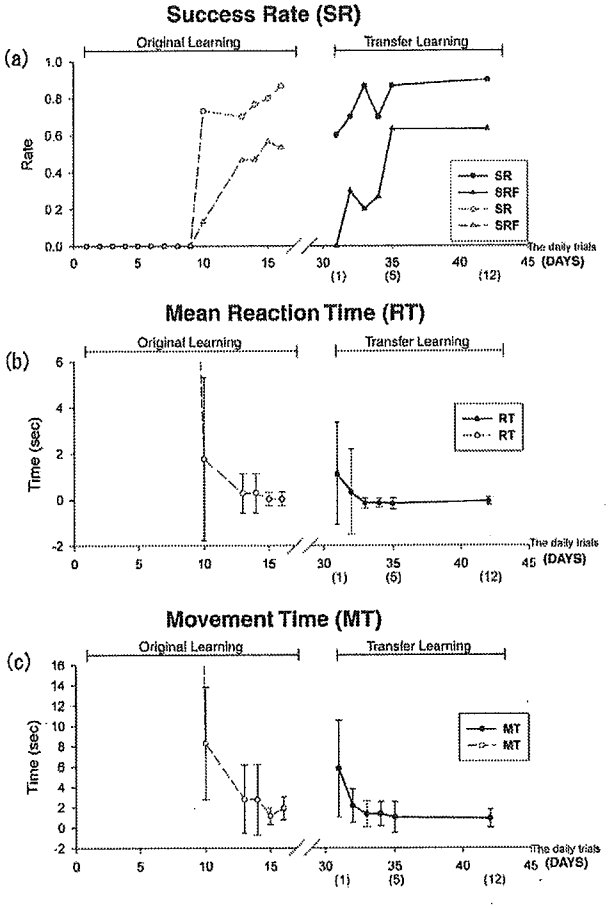

Fig. 1. Learning curves of OL and TL. (a) SR or SRF in OL and TL. Day 1 of TL is shown as "(1)" in parentheses, indicating the start of TL 1 month after that of OL. (b) RT on sequential movement. (c) MT toward a target. Data of RT and MT represent mean ± SD. Numerals along the abscissa and those in parentheses show days when data were obtained.

detected, continuing for 120 s. Interscan interval was 11 min. Tasks were started about 10 s before tracer administration using a reproducible automated water generator (A&RMC, Melbourne, Australia), and the monkeys continued performing the tasks for 90 s. M_1 and M_2 were scanned during the two tasks, and thus all 24 PET images were counterbalanced (tool-use task 12, control task 12). The monkeys underwent MRI scans (Philips GYROSCAN Interna 1.5 Tesla; 3D-T_1 mode, TR 30 ms, TE 6 ms, 60 slices; 1 mm thickness).

Reconstructed images were preprocessed and analyzed with Statistical Parametric Mapping software (SPM 99). Each image was smoothed with isotropic Gaussian kernel (4.5 mm). Global activity for each scan was corrected by grand mean scaling, using analysis of covariance (ANCOVA) for global normalization. Statistical results were based on single-voxel T threshold of 3.53 (corresponding to $P < 0.001$, uncorrected for multiple comparisons). After MRI volumes were coregistered with PET data, each matched pair of MRI and PET data sets was displayed using 3D BrainStation (Loats Associates, Inc., Westminster, MD).

Regions of significant rCBF changes are summarized in

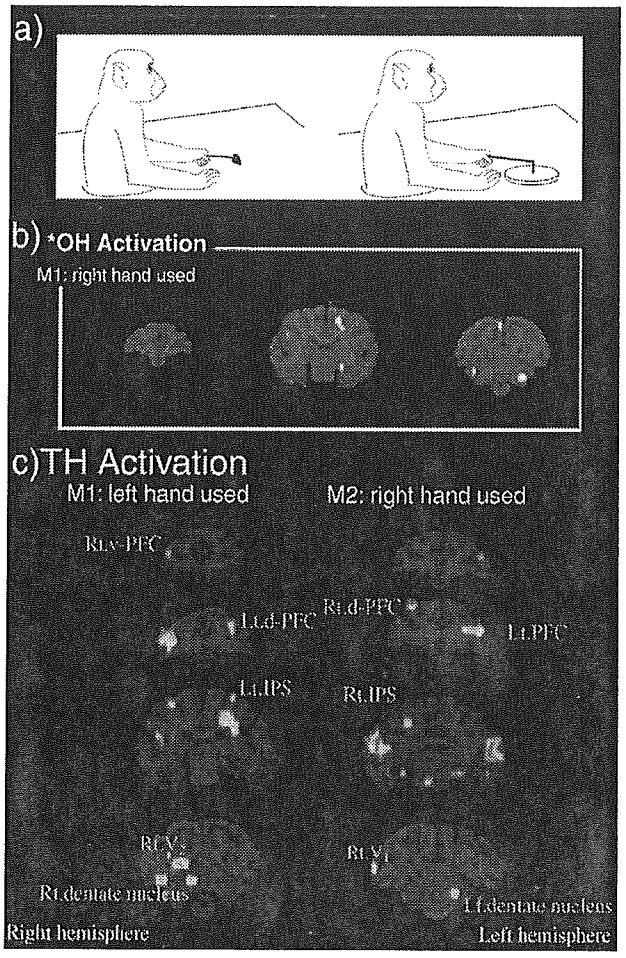

Fig. 2. (a) Task design for PET. (a-1; left) Tool-use task, (a-2; right) Control task. (b) OH activation as basis of comparison with TH activation. OH activation previously reported was modified [12]. Note there was no activity in PFC. (c) TH activation for comparison of conditions of tool-use task vs. control task (tool > control). Coronal views of TH activation in PFC, IPS, and cerebellum (orthogonal to AC–PC line).

Fig. 2c and Table 1. Within TH activation, there were greater activities in the bilateral prefrontal cortex (PFC; area 9/46 dorsal and ventral complex), bilateral IPS, bilateral IT, right primary visual cortex and cerebellum (near the dentate nucleus) contralateral to TH. TH activation was consistent between the two monkeys.

TH activation was not symmetrical with OH activation (Fig. 2b,c). Supporting our results, a recent study claimed that the bilateral frontal cortices are crucial for transfer of procedural visuomotor skill [1].

Our earlier study aimed to detect the brain regions underlying tool-use, and near consistency of activation between two monkeys was observed [12]. Differences in activity may be rather related to the data being composed of OH activation from M_1 and TH activation from M_2. To test the above hypothesis, we re-analyzed the earlier M_2 data by adding six PET images. As a result, the consistency in TH activation could strengthen our hypothesis, although in the earlier analysis TH activation was absent in the PFC, IPS ipsilateral to TH, and visual cortex. Presumably, the absence of activities may be related to a lack of statistical power in terms of insufficient numbers of PET images for testing the hypothesis, different from that in the earlier study.

Tool-use skill would produce a 'motor engram' specific for the learned hand, and be stored as procedural memory. The cerebellum may be essential for procedural memory [2, 6]. A recent monkey study investigated the effect of focal inactivation in the dentate nucleus on cerebellar function [9], claiming that the dentate nucleus ipsilateral to the learned hand should be specialized for storage and/or retrieval of an established motor skill. Our results showed cerebellar activation ipsilateral to the learned hand initially during tool-use with TH. Cerebellar projections to the opposite dorsal PFC support the view that the cerebellum may modulate the executive process such as cognitive flexibility [8,10]. Hence, we can predict that OL derived-procedural memory may mediate TL by its retrieval and be applied to TL, presumably by means of modification of procedural memory for OH.

Interestingly, bilateral IPS regions and early visual cortex are involved in manipulation of mental representation such as mental rotation [7]. Furthermore, our recent

Table 1
TH activation (Subtracted Image; tool > control)[a]

Region	T value (Z score)
(M1: LH used, Transfer Direction: R to L)	
R prefrontal cortex (PFC: ventral and dorsal area 9/46)	5.23 (4.14)
L dorsal PFC	2.52 (2.33)
R cerebellum (dentate nucleus)	3.14 (2.81)
R lateral cerebeller hemisphere	4.72 (3.85)
pre-SMA (presupplementary motor area)	2.80 (2.55)
R dorsal premotor cortex (PM)	3.34 (2.96)
L M_1 (primary motor cortex)	3.56 (3.11)
R intraparietal sulcus (IPS)	3.16 (2.82)
L IPS	3.66 (3.18)
R inferotemporal cortex (IT)	2.78 (2.53)
L IT	3.50 (3.07)
RV_2 (area 18)	4.11 (3.48)
(M2: RH used, Transfer Direction: L to R)	
L PFC (ventral and dorsal area 9/46)	4.22 (3.55)
R dorsal PFC	4.02 (3.42)
R ventral PLC	4.23 (3.56)
L cerebellum (dentate nucleus)	4.24 (3.57)
L ventral PM	3.03 (2.73)
R dorsal PM	3.22 (2.87)
R IPS	2.97 (2.68)
L IPS	3.56 (3.11)
L hippocampus	3.92 (3.35)
L IT	3.38 (2.99)
R IT	4.23 (3.56)
RV_1 (area 17)	4.87 (3.94)

[a] Focal regions of signilicantly ($P < 0.001$, uncorrected for multi-comparison) increased regional cerebral blood flow during tool-use task (relative to control task) with TH. LH, left hand: RH, right band; V, primary visual cortex.

studies demonstrated that visual-tactile bimodal neurons in the monkey IPS region might code the representation of 'body image' [3,4,11]. The visual response could be modified as if incorporating the tool into a body-part during tool-use [3]. If body image may be engaged in the motor action plan of tool-use, body image should be closely related to motor engram of tool-use.

Taken together, we propose that the interaction among PFC, cerebellum and IPS may be engaged in producing and manipulating a motor engram of tool-use shared by both hands in terms of modifying OH-specific procedural knowledge.

Acknowledgements

This work was supported by a grant from the Japanese Ministry of Education, Culture, Sports, Science and Technology.

References

[1] E. de Guise, M. del Pesce, N. Foschi, A. Quattrini, I. Papo, M. Lassonde, Callosal and cortical contribution to procedural learning, Brain 122 (1999) 1049–1062.
[2] D. Flament, J.M. Ellermann, S.G. Kim, K. Ugurbil, T.J. Ebner, Functional magnetic resonance imaging of cerebellar activation during the learning of a visuomotor dissociation task, Hum. Brain Mapp. 4 (1996) 210–226.
[3] A. Iriki, M. Tanaka, Y. Iwamura, Coding of modified body schema during tool use by macaque postcentral neurons, NeuroReport 7 (1996) 2325–2330.
[4] A. Iriki, M. Tanaka, S. Obayashi, Y. Iwamura, Self-images in the video monitor coded by monkey intraparietal neurons, Neurosci. Res. 40 (2001) 163–173.
[5] H. Ishibashi, S. Hihara, M. Takahashi, T. Heike, T. Yokota, A. Iriki, Tool-use learning selectively induces expression of brain-derived neurotrophic factor, its receptor trkB, and neurotrophin 3 in the intraparietal cortex of monkeys, Cogn. Brain Res. 14 (2002) 3–9.
[6] S.G. Kim, K. Ugurbil, P.L. Strick, Activation of a cerebellar output nucleus during cognitive processing, Science 265 (1994) 949–951.
[7] S.M. Kosslyn, A. Pascual-Leone, O. Felician, S. Camposano, J.P. Keenan, W.L. Thompson, G. Ganis, K.E. Sukel, N.M. Alpert, The role of area 17 in visual imagery: convergent evidence from PET and rTMS, Science 284 (1999) 167–170.
[8] H.C. Leiner, A.L. Leiner, R.S. Dow, The underestimated cerebellum, Hum. Brain Mapp. 2 (1995) 244–254.
[9] X. Lu, O. Hikosaka, S. Miyachi, Role of monkey cerebellar nuclei in skill for sequential movement, J. Neurophysiol. 79 (1998) 2245–2254.
[10] F.A. Middleton, P.L. Strick, Cerebellar projections to the prefrontal cortex of the primate, J. Neurosci. 21 (2001) 700–712.
[11] S. Obayashi, M. Tanaka, A. Iriki, Subjective image of invisible hand coded by monkey intraparietal neurons, NeuroReport 11 (2000) 3499–3505.
[12] S. Obayashi, T. Suhara, K. Kawabe, T. Okauchi, J. Maeda, Y. Akine, H. Onoe, A. Iriki, Functional brain mapping of monkey tool use, Neuroimage 14 (2001) 853–861.

Psychiatry and Clinical Neurosciences (2003), **57**, 433–440

Regular Article

Determining vulnerability to schizophrenia in methamphetamine psychosis using exploratory eye movements

TOMOKO MIKAMI, MD,[1,2,3] NOBUYA NARUSE, MD,[2] YOICHI FUKURA, MD,[3] HIROMI OHKUBO, MD,[3] TATSUNOBU OHKUBO, MD,[3] MASATO MATSUURA, MD,[3] HIROBUMI MORIYA, MD,[2] TORU NISHIKAWA, MD, PhD[1] AND TAKUYA KOJIMA, MD, PhD[3]

[1]Section of Psychiatry and Behavioral Science, Graduate School of Tokyo Medical and Dental University, Tokyo, [2]Saitama Prefecture Government Psychiatric Hospital, Saitama and [3]Department of Neuropsychiatry, Nihon University, School of Medicine, Tokyo, Japan

Abstract Patients with methamphetamine (MAP) psychosis whose psychotic symptoms continued after MAP withdrawal were observed at Saitama Prefecture Government Psychiatric Hospital. The purpose of the present study was to ascertain whether some of these MAP psychosis subjects have a vulnerability to schizophrenia. Forty-eight patients with MAP psychosis were divided into three groups based on clinical course: transient type, prolonged type and persistent type. Furthermore, the patients with the persistent type were divided into two groups: one group were moderately disturbed in social adaptive functioning and had Global Assessment Functioning scale (GAF) points >50, and the other group consisted of those who were severely disturbed in social adaptive functioning and who had GAF points of ≤50. These MAP patients were tested for exploratory eye movements, which are the vulnerability marker of schizophrenia, and were compared with 30 patients with schizophrenia and 30 healthy control subjects. The responsive search score of the severely disturbed group of patients of the persistent type was lowest, significantly lower than those of the transient type and the healthy controls. It did not differ from that of the schizophrenic subjects. These results suggest that the severely disturbed group of patients with the persistent type of MAP psychosis have a vulnerability to schizophrenia.

Key words exploratory eye movements, Global Assessment Functioning Scale, methamphetamine psychosis, schizophrenia, vulnerability.

INTRODUCTION

Methamphetamine (MAP) psychosis is characterized by a paranoid psychosis with a delusion of persecution, and auditory and visual hallucinations. These cross-sectional features are indistinguishable from those of schizophrenia, and MAP has been considered as a subject for the experimental model of schizophrenia. While most patients with MAP psychosis display the positive symptoms of schizophrenia, many of them have only slight negative symptoms. Few of them progress to the characteristic schizophrenic defect state despite many relapses. This suggests that MAP psychosis has different etiological factors from schizophrenia. The difference in morbid risk between MAP psychosis and schizophrenia has been demonstrated and it reinforces this view.

The first report of amphetamine psychosis by Connell found that amphetamine psychosis is due to the direct pharmacological action of amphetamine and is never prolonged after excretion in the urine.[1] Amphetamine is closely related chemically to MAP.[2] However, in Japan, where there is an epidemic of

Correspondence address: Takuya Kojima, Department of Neuropsychiatry, Nihon University School of Medicine, 30-1 Oyaguchi-Kamimachi, Itabashi-ku, Tokyo 173-8610, Japan.
Email: kojima@med.nihon-u.ac.jp

Received 11 November 2002; revised 9 January 2003; accepted 14 January 2003.

MAP abuse and a large number of MAP psychosis cases due not to multiple drugs but to MAP abuse, many reports indicate the existence of MAP psychosis patients whose psychotic symptoms continue after the excretion of MAP, sometimes for more than several months.[3–8] It is hypothesized that some of the MAP patients as described here have a vulnerability to schizophrenia.

A psychophysiological method using two kinds of eye movements (smooth pursuit and exploratory eye movements) appeared to be a strong candidate as a vulnerability marker of schizophrenia. Holzman *et al.* substantiated a dysfunction of smooth pursuit eye movements in schizophrenic patients.[9] In addition, they found disruptions of smooth pursuit eye movements in 52% of recent and 86% of chronic schizophrenic patients as well as in 44% of their relatives. Such deviant eye tracking in pursuit eye movements, however, was also seen in patients with other psychiatric diseases, particularly in patients with mood disorders.[10] These findings suggest that abnormal smooth pursuit eye movements could serve as a vulnerability marker of schizophrenia, but would not become a specific marker for schizophrenia.

Kojima *et al.* reported that schizophrenic subjects (and not only chronic but also acute and remitted), performed less exploratory eye movements in response to verbal stimuli (i.e. the responsive search score; RSS).[11] Obayashi *et al.* also found that neuroleptic medication had little effect on RSS.[12] There is another report that reinforces this.[13] Gender, and age were founded to have no influence on the RSS.[14] Further studies indicated that healthy parents and siblings of schizophrenic patients have a lower RSS than healthy controls.[14–17] The depressed patients with a family history of schizophrenia demonstrated a lower RSS than the patients without a family history.[17] Also, Hagiwara *et al.* noted that with an increase in the number of first-degree schizophrenic family members of schizophrenic subjects, their RSS became lower.[17] Matsushima *et al.* studied monozygotic twins, discordant and concordant for schizophrenia. The RSS of the discordant twin group elucidated a higher value than those of the concordant twins.[18] Matsushima *et al.* reported that the RSS and the number of eye fixations (NEF) discriminate schizophrenic patients from patients without schizophrenia and healthy subjects with a sensitivity of 76.7% and a specificity of 81.4%.[19] Therefore, exploratory eye movements are considered to be not only a disease-specific marker but also a vulnerability marker of schizophrenia.

In the present study, we investigated the relationship between MAP psychosis and schizophrenia using exploratory eye movements.

MATERIALS AND METHODS

Subjects

Forty-eight patients with MAP psychosis (34 male and 14 female; mean age at the time of testing 33.0 ± 8.5 years), who were 32 inpatients and 16 outpatients at the Saitama Prefecture Government Psychiatric Hospital were included in the study. The patients with MAP psychosis were divided into three groups using the classification of Sato *et al.*,[20] according to the duration of psychotic symptoms: transient type (<10 days), prolonged type (10–31 days) and persistent type (>1 month). The transient type (TR type) is acute MAP intoxication, which is due to direct action by MAP and which rapidly discontinues after the urinary excretion of MAP. In contrast, the persistent type (PE type) is a type of MAP psychosis reported in Japan in which the psychotic state continues for >1 month, and often for several years. The prolonged type (PR type) is the medium type. All of the subjects who were classified as the PR type and the PE type were inpatients and their non-use of MAP was confirmed. The diagnosis was assigned by the Structured Clinical Interview for axis I disorders of *Diagnostic and Statistical Manual of Mental Disorders* (4th edn; DSM-IV).[21] The TR and PR type belong to 'amphetamine-induced psychotic disorder' and the PE type belongs to 'schizophreniform disorder' or 'schizophrenia' according to the DSM-IV criteria.

Thirty age-matched patients (20 male and 10 female; 34.8 ± 8.8 years) met the DSM-IV criteria for schizophrenia without a past history of MAP use, and 30 age-matched healthy subjects (21 male and nine female; 31.5 ± 5.3 years) were selected as the controls. There was no significant difference in gender between these three groups ($\chi^2 = 0.150$, d.f. = 2, $P = 0.6981$). The subjects who had any neurological findings including eye movement dysfunction were excluded.

The clinical information was confirmed by interview with the patients and their families, and clinical records. The mean years of full-time education and family history of each group were investigated. The mean education time of the MAP psychosis subjects was 10.3 ± 1.5 years (Table 1), and was low for the Japanese education system. The schizophrenic subjects and healthy subjects had a similar mean education time, and there was a significant difference between the MAP psychosis subjects and healthy controls ($P < 0.01$), and between the schizophrenic subjects and healthy controls ($P < 0.05$). The family history of schizophrenia was investigated as far as third-degree relatives. All the healthy controls had no history of psychiatric disorder including substance use disorder, and no family history of schizophrenia as far back as their third-degree relatives. A total of 18.8% of the

Table 1. Demographic characteristics of the MAP psychosis, schizophrenia, and healthy control groups

Groups	MAP psychosis patients	Transient	Prolonged	Persistent	LD group	SD group	Schizophrenic subjects	Healthy controls
Subjects (n)	48	16	14	18	11	7	30	30
Mean age (years, mean ± SD)	33.0 ± 8.5	32.9 ± 8.1	31.9 ± 10.8	34.0 ± 7.2	34.5 ± 5.0	33.1 ± 10.1	34.8 ± 8.8	31.5 ± 5.3
Gender (M:F)	34:14	9:7	9:5	16:2	10:1	6:1	20:10	21:9
Mean years of full-time education (mean ± SD)	10.3 ± 1.5*	10.8 ± 1.7	10.5 ± 1.5	9.7 ± 1.2*	9.5 ± 0.8*	10.0 ± 1.7	10.8 ± 1.9**	11.9 ± 0.5
Dose of medication at the test (chlorpromazine equivalents) (mg, mean ± SD)	1016 ± 1353	488 ± 556	596 ± 520	1810 ± 1872†‡	1610 ± 1416	2125 ± 2531†	1363 ± 899	–
Mean duration of illness (years)	6.0 ± 5.3§	6.2 ± 6.2§	3.7 ± 3.3§	7.6 ± 5.4¶	7.2 ± 5.5	8.0 ± 5.6	14.1 ± 9.3	–

Gender for three groups ($\chi^2 = 0.150$, d.f. = 2, $P = 0.6981$).
* $P < 0.01$ *vs* healthy controls (ANOVA with Scheffé); ** $P < 0.05$ *vs* healthy controls (ANOVA with Scheffé); † $P < 0.05$ *vs* transient type (ANOVA with Scheffé); ‡ $P < 0.05$ *vs* prolonged type (ANOVA with Scheffé); § $P < 0.01$ *vs* schizophrenia (ANOVA with Scheffé); ¶ $P < 0.05$ *vs* schizophrenia (ANOVA with Scheffé).

MAP psychosis subjects and 33.3% of the schizophrenic subjects had a family history of schizophrenia ($\chi^2 = 2.131$, $P = 0.1444$).

The daily neuroleptic dose at the time of examination and the mean duration of illness of each patient with MAP psychosis and schizophrenia were evaluated. There was no significant difference in the neuroleptic dose of three groups of MAP psychosis and schizophrenic subjects. However, in the PE-type patients, it was significantly higher than that of the TR-type patients ($P < 0.05$). The mean duration of illness was designated as the duration between the occurrence of the psychosis and examination. The MAP psychosis subjects had a significantly shorter duration of illness than the schizophrenic subjects ($P < 0.01$).

Procedure

The procedure was carried out as described by Kojima *et al.*[22] Both the patients with MAP psychosis and schizophrenia, and all the healthy subjects were willing to give informed consent. Each subject took a seat in a dark quiet room equipped with an eye-mark recorder (nac VII-type, Tokyo, Japan), a device that detects corneal reflections made by infrared light. Three horizontal S-shaped figures as shown in Fig. 1 were projected individually onto a screen located 1.5 m directly in front of the subject. While the subject looked at the figure, his/her eye fixation points were recorded by the eye-mark recorder and videotaped. The target figure pattern was a horizontal S-shape with two bumps; the left bump was above the horizontal line and the right bump was beneath the horizontal line. One of the comparison figures was different from the target figure at one point, in which the left bump moved beneath the left upper curve (comparison fig. 1). The other figure differed from the target, which had no bump (comparison fig. 2). The examination procedure was as follows.

(1) Each subject was shown the target S-shaped figure (Fig. 1a) for 15 s.

(2) The subject was then asked to draw the figure from memory immediately after viewing it.

(3a) The subject was instructed to compare a figure with the first target figure and was shown the comparison figure 1 (Fig. 1b left) for 15 s.

(3b) Directly after the 15 s had elapsed and with the figure still showing, the subject was asked if it differed from the target figure, and if it did so, how it differed.

(3c) After the reply had been given and while the figure was still showing, the subject was then asked 'Are there any other differences?' (This question was repeated until the subject stated that there were no differences present.)

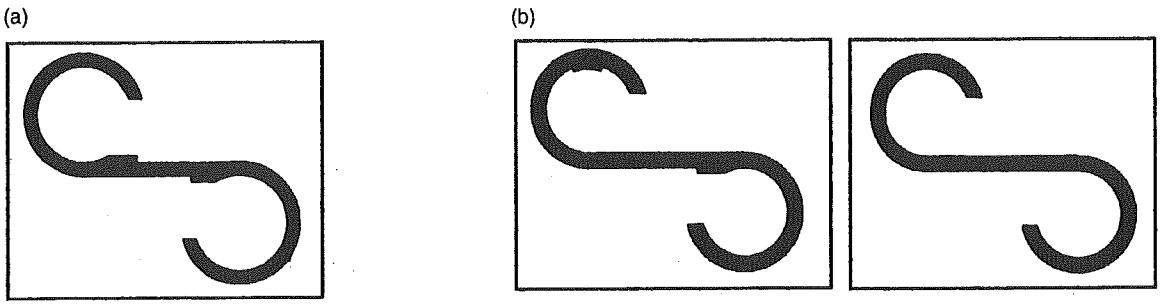

Figure 1. Horizontal S-shaped figures. (a) Target figure. (b) Comparison figure 1 (left) and 2 (right).

Steps 3a–c were repeated for a figure the same as the target and the comparison figure 2 (Fig. 1b right).

(4) The subject was then told to look at the target figure carefully in order to draw it again and reshow it for 15 s.

(5) Finally, the subject was asked to draw the target figure from memory a second time.

Exploratory eye movements were recorded on videotape using the eye mark recorder during steps 1, 3 and 4.

Measurement

The recorded tapes were analyzed with a computerized analyzing system and slow-motion replay. We analyzed the elementary components and responsive search score.

Elementary components of eye movements

We analyzed NEF and the total eye scanning length (TESL) during the subject's first 15-s viewing of the target figure in step 2.

Responsive components

The two comparison figures were each divided into seven sections. The number of sections upon which the subject's eye fixed one or more times were counted for 5 s immediately after the final question, 'Are there any other differences?' in step 3c, and was measured as the responsive search score (RSS).

Evaluation of psychiatric symptoms

Two trained research psychiatrists performed the Brief Psychiatric Rating Scale (BPRS) for the MAP psychosis subjects and schizophrenic patients, and scored the positive symptom subscale (hostility, suspiciousness, hallucinatory behavior, unusual thought) and the negative symptom subscale (emotional withdrawal, motor retardation, blunted affect).[23]

Social adaptive functioning level

The MAP psychosis subjects and the schizophrenic subjects were evaluated for their level of social adaptive functioning using the Global Assessment of Functioning Scale (GAF) of DSM-IV at discharge or when the symptoms had stabilized. The GAF was rated on the psychosocial functioning from 0 to 100 points, and the persistent type patients of MAP psychosis were classified into two groups. One was the lightly disturbed group (LD group) with a GAF >50, and the other was the severely disturbed group (SD group) with a GAF of ≤50. In the GAF range of 51–60 points, the assessment scale was 'moderate difficulty in social, occupational, or school functioning (e.g. few friends, conflicts with coworkers, unable to complete work assignments, unsatisfactory work performance)', and in the range 49–50 points the assessment scale was 'serious impairment in social, occupational, or school functioning (e.g. no friends, unable to keep a job at expected or prior level of performance)'. Therefore, this measure differentiated patients who had mild symptoms and adequate social functioning from those who had severe symptoms and poor social functioning. We dichotomized the GAF to minimize problems of inaccuracies due to small differences in the GAF levels.

Statistical analysis

A statistical analysis was carried out using a one-way ANOVA with one between-group factor followed by post hoc comparisons (Scheffé *F*-test). The difference was considered statistically significant when $P<0.05$.

RESULTS

Global Assessment of Functioning Scale

One-way ANOVA showed significant differences between the GAF scores of the six groups ($F(5,102)=90.421$, $P<0.0001$; Table 2). The MAP psychosis subjects had a significantly higher GAF level

Table 2. The BPRS at the test, GAF at the time symptoms stable, and family history in the groups of MAP psychosis and schizophrenia

Groups	MAP psychosis patients	Transient	Prolonged	Persistent		Schizophrenic subjects
				LD group	SD group	
BPRS						
Total scores	10.5±5.0*	8.9±4.2*	11.1±4.5*	8.7±3.8*	16.0±6.2**	31.2±17.0
Subscale for Positive Symptoms	1.7±2.1*	1.4±2.3*	1.3±1.2*	1.5±1.1*	3.3±3.6**	7.3±3.8
Subscale for Negative Symptoms	1.4±2.3*	0.0*	1.1±2.7*	1.9±1.4*	4.3±2.6	7.5±3.6
GAF	54.3±7.8*	57.6±4.7*	54.0±11.3**	55.2±2.3**	46.1±5.7	42.7±14.8
Family history of schizophrenia	9 (18.8%)	2 (12.5%)	3 (21.4%)	2 (18.2%)	2 (28.6%)	10 (33.3%)
No family history	39 (81.3%)	14 (87.5%)	11 (78.6%)	9 (81.8%)	5 (71.4%)	20 (66.7%)

Family history for MAP psychosis subjects and schizophrenic subjects ($\chi^2=2.131$, d.f.=1, $P=0.1444$), four groups of MAP psychosis and schizophrenic subjects ($\chi^2=2.893$, d.f.=4, $P=0.5759$).

* $P<0.01$ *vs* schizophrenia (ANOVA with Scheffé); ** $P<0.05$ *vs* schizophrenia (ANOVA with Scheffé).

MAP, methamphetamine; LD, lightly disturbed; SD, severely disturbed; BPRS, Brief Psychiatric Rating Scale; GAF, Global Assessment of Functioning.

than the schizophrenic subjects ($P<0.01$). Comparing the three type of patients of MAP psychosis and schizophrenic subjects, the TR- and PR-type patients had significantly higher GAF levels than the schizophrenic subjects (*vs* TR type $P<0.01$; *vs* PR type $P<0.05$). There was no significant difference between the GAF scores of the PE type and schizophrenic subjects. The PE-type patients were then divided into two groups. The LD group consisted of 11 patients (10 male and one female), and the SD group consisted of seven patients (six male, one female). The LD group had a significantly higher GAF score than the schizophrenic subjects ($P<0.05$), while the SD group had no significantly different GAF score from the schizophrenic subjects.

Brief Psychiatric Rating Scale

There was significant difference in each BPRS total score, positive symptom scale points and negative symptom scale points between the six groups (total BPRS score: $F(5,102)=34.480$, $P<0.0001$; positive symptom scale points: $F(5,102)=41.853$, $P<0.0001$; negative symptom scale points: $F(5,102)=31.021$, $P<0.0001$; Table 2). Post-hoc test revealed that the patients of MAP psychosis had a significantly lower BPRS total score, positive symptom scale points, and negative symptom scale points than the schizophrenic subjects (each score $P<0.01$). When comparing the four groups of MAP psychosis and schizophrenic subjects, the total score was significantly lower for each group of MAP psychosis than for the schizophrenic subjects (*vs* TR type, PR type and LD group, $P<0.01$; *vs* SD group, $P<0.05$). The positive symptom scale points were also similarly lower for each group of MAP psychosis than for schizophrenic subjects (*vs* TR type, PR type and LD group, $P<0.01$; *vs* SD group, $P<0.05$). For the negative symptom scale points, the TR type, PR type and LD group had significantly lower points than the schizophrenic subjects (*vs* each group, $P<0.01$), but no significant difference was found between the patients of the SD group and the schizophrenic subjects.

Exploratory eye movements

There was significant difference in each RSS score, NEF and TESL between the MAP psychosis subjects, the schizophrenic subjects and the healthy subjects (RSS score: $F(5,102)=23.889$, $P<0.0001$; NEF, $F(5,102)=13.635$, $P<0.0001$; TESL: $F(5,102)=18.973$, $P<0.0001$; Table 3). The schizophrenic subjects had a significantly lower RSS score than the healthy subjects ($P<0.01$). Also, the MAP psychosis subjects had an

Table 3. Values of NEF, TESL, RSS in four groups of MAP psychosis, schizophrenia, and healthy controls

Groups	MAP psychosis	Transient	Prolonged	Persistent		Schizophrenic subjects	Healthy controls
				LD group	SD group		
NEF	31.3±7.9†	33.4±8.3	31.4±4.3‡	31.3±8.2†	26.3±11.1†	31.6±10.0†	40.8±7.4
TESL	457.9±194.4†	520.2±244.8‡	456.0±115.9†	457.0±153.9‡	320.3±212.7†	478.7±237.7†	727.9±158.0
RSS	9.0±1.8*†	9.7±0.2*§	9.1±1.3*‡¶	9.2±1.9**	6.6±1.5†	7.0±1.5†	10.9±1.7

*$P<0.01$ *vs* schizophrenia (ANOVA with Scheffé); **$P<0.05$ *vs* schizophrenia (ANOVA with Scheffé); †$P<0.01$ *vs* healthy controls (ANOVA with Scheffé); ‡$P<0.05$ *vs* healthy controls (ANOVA with Scheffé); §$P<0.01$ *vs* SD group (ANOVA with Scheffé); ¶$P<0.05$ *vs* SD group (ANOVA with Scheffé).

NEF, number of eye fixations; TESL, total eye scanning length; RSS, responsive search scores; MAP, methamphetamine; LD, lightly disturbed; SD, slightly disturbed.

RSS score that was significantly lower than that of the healthy subjects ($P<0.01$), but significantly higher than the schizophrenic subjects ($P<0.01$). The NEF was significantly less for the MAP psychosis subjects than for the healthy subjects ($P<0.01$), and TESL was significantly shorter for the MAP psychosis subjects than for the healthy subjects ($P<0.01$). However, there was no significant difference between the MAP psychosis subjects and schizophrenic subjects for both NEF and TESL.

Furthermore, for the four groups of the MAP psychosis, schizophrenic subjects and healthy subjects, there was significant difference in each RSS score, NEF and TESL (RSS score: $F(5,102)=21.250$, $P<0.0001$; NEF: $F(5,102)=6.174$, $P<0.0001$; TESL: $F(5,102)=8.744$, $P<0.0001$). The RSS was significantly lower for the patients of the PR type, SD group and schizophrenic subjects than the healthy subjects (*vs* PR type, $P<0.05$; *vs* SD group and schizophrenic subjects, $P<0.01$), and was significantly higher for the patients of the TR type, PR type and LD group than the schizophrenic subjects (*vs* TR and PR types, $P<0.01$; *vs* LD group, $P<0.05$). The TR- and PR-type patients had a significantly higher RSS than the SD group (*vs* TR type, $P<0.01$; *vs* PR type, $P<0.05$). However, the TR-type patients and LD group had no significantly different RSS from the healthy subjects, and no significant difference was found between the RSS of the SD group and schizophrenic subjects. The NEF was significantly lower for the patients of the PR type, LD group, SD group and schizophrenic subjects than for the healthy subjects (*vs* PR type, $P<0.05$; *vs* LD group, SD group and schizophrenic subjects, $P<0.01$), and there was no significant difference between the NEF of the TR-type patients and healthy subjects. As for TESL, no significant difference was found between each group of MAP psychosis and the schizophrenic subjects. All four groups of the MAP psychosis and schizophrenic subjects had a significantly lower TESL than the healthy subjects (*vs* TR type and LD group, $P<0.05$; *vs* PR type, SD group and schizophrenic subjects, $P<0.01$), but there was no significant difference between each group of MAP psychosis and schizophrenic subjects.

DISCUSSION

Global Assessment of Functioning and Brief Psychiatric Rating Scale

The SD group of the PE type with MAP psychosis, who had a low social adaptive level, showed no significant difference in negative symptom scale points compared with the schizophrenic subjects. This means that among the MAP psychosis subjects, the SD group was different from the TR- and PR-type patients, whose psychotic symptoms disappear sooner after discontinuation of MAP. The SD group had not only prolonged delusions and hallucinations, but also those symptoms similar to the negative symptoms of schizophrenia, no matter whether the delusions and hallucinations had stopped or were prolonged. Residual syndromes observed during the abstinence from MAP were classified by Konuma into five types: residual neurosis; positive symptom; residual depressive; negative symptom; and personality disorder; and shifts among the four former types were noted.[6] The SD group is thought to have both the characteristics of the positive and negative symptom types.

Exploratory eye movements

In Europe and the USA, MAP psychosis is regarded as acute psychosis that results from direct pharmacological action, while 'chronic' MAP psychosis is generally induced schizophrenia,[24,25] whereas clinical and animal studies of MAP suggest that the psychosis develops on the basis of brain damage that occurs from

repetitive and chronic uses of MAP.[4,5,7,20] This argument is ongoing.

In the present study the RSS of the patients of MAP psychosis was higher than that of the schizophrenic subjects, and lower than that of the healthy subjects. This finding suggests that there is a possibility that the patients of MAP psychosis include a few who have a vulnerability to schizophrenia. Kojima *et al.* previously studied amphetamine psychosis using exploratory eye movements.[26] They reported that amphetamine psychosis subjects had fewer NEF, similar to schizophrenic subjects, but they had a high RSS, which is in distinct contrast to schizophrenic subjects. In contrast, the RSS of MAP psychosis subjects in the current study was lower than that of the schizophrenic subjects. The subjects of MAP psychosis in the study by Kojima *et al.* were not divided into classes by clinical course, so it is possible that the majority of the subjects corresponded to the TR type of MAP psychosis, which might be a reason for the contrast between the results of the two studies. The present study, dividing the MAP psychosis into four groups, indicated that the RSS of the SD group patients was the lowest, significantly different from that of the TR-type patients, and did not differ from that of the schizophrenic subjects, whereas the RSS of the TR-type patients was highest in those four groups, there was no difference between the RSS of the TR type and the healthy subjects. This raised some question if exploratory eye movements were reflected in the GAF level, but the schizophrenic subjects had no significant correlation between GAF level and RSS score ($r=0.378$, $P=0.0417$) as analyzed using Spearman's rank correlation test, although the GAF level of the MAP psychosis subjects had significant correlation with RSS score ($r=0.520$, $P<0.0001$). These results suggest that the TR-type patients of MAP psychosis have little vulnerability to schizophrenia and the effects of pharmacological action may play a more important role. In contrast, it was suggested that the SD group of patients of the PE type includes subjects who have a vulnerability to schizophrenia. The high percentage with a family history of schizophrenia in the SD group patients reinforces their diathesis for schizophrenia.

Repeated administrations of MAP are known to augment the susceptibility to the psychotic state, which result in a psychotic relapse following a single low dose of MAP reuse after a long period of abstinence. This sensitization phenomenon explains part of these findings. Neurochemical studies also indicated that amphetamine-induced dopamine release was enhanced in the striatum of sensitized animals[27] and patients with schizophrenia.[28] Sato suggested that enhanced dopamine release may be related to psychotic vulnerability in both schizophrenia and MAP psychosis.[29] In any case the extracting of the group with vulnerability of schizophrenia from the patients with MAP psychosis was considered to be very important. Clinical information such as duration of MAP usage and relapse without MAP reuse is excluded from the present study because the illegality of drug abuse and the antisocial nature of patients made it difficult to obtain reliable information about them. A further study of schizophrenia and MAP psychosis is needed.

ACKNOWLEDGMENTS

The present study was supported by a grant No. H13-pharmaceutical and medical safety-040 from the Ministry of Health and Welfare, Japan. We would like to thank Professor Mitsumoto Sato for his support.

REFERENCES

1. Connell PH. *Amphetamine Psychosis*. Oxford University Press, London, 1958.
2. Melega WP, Williams AE, Schmitz DA *et al.* Pharmacokinetic and pharmacodynamic analysis of the actions of D-amphetamine and D-methamphetamine on the dopamine terminal. *J. Pharmacol. Exp. Ther.* 1995; **274**: 90–96.
3. Tatetsu S, Goto A, Fujiwara T. *The Methamphetamine Psychosis.* Igakushoin, Tokyo, 1956 (in Japanese).
4. Tomiyama G. Chronic schizophrenia-like states in methamphetamine psychosis. *Jpn. J. Psychiatry Neurol.* 1990; **44**: 531–539.
5. Sato M. A lasting vulnerability to psychosis in patients with previous methamphetamine psychosis. *Ann. NY Acad. Sci.* 1992; **654**: 160–170.
6. Konuma K. Use and abuse of amphetamines in Japan. In: Cho AK, Segal DS (eds). *Amphetamine and its Analogs*. Academic Press, San Diego, 1994; 415–435.
7. Iwanami A, Sugiyama A, Kuroki N *et al.* Patients with methamphetamine psychosis admitted to psychiatric hospital in Japan. *Acta Psychiatr. Scand.* 1994; **89**: 428–432.
8. Flaum M, Schultz SK. When does amphetamine-induced psychosis become schizophrenia? *Am. J. Psychiatry* 1996; **253**: 812–815.
9. Holzman PS, Proctor LR, Levy DL *et al.* Eye-tracking dysfunctions in schizophrenic patients and their relatives. *Arch. Gen. Psychiatry* 1974; **31**: 143–151.
10. Shagass C, Amadeo M, Overton DA. Eye tracking performance in psychiatric patients. *Biol. Psychiatry* 1974; **9**: 245–260.
11. Kojima T, Matsushima E, Nakajima K *et al.* Eye movement in acute, chronic and remitted schizophrenics. *Biol. Psychiatry* 1990; **27**: 975–989.
12. Obayashi S, Matsushima E, Okbo Y *et al.* Relationship between exploratory eye movements and clinical course in schizophrenic patients. *Eur. Arch. Psychiatry Clin. Neurosci.* 2001; **251**: 211–216.

13. Hori Y, Fukuzako H, Sugimoto Y, Takigawa M. Eye movements during the Rorschach test in schizophrenia. *Psychiatry Clin. Neurosci.* 2002; **56**: 409–418.
14. Xia ML, Takahashi S, Tanabe E *et al.* Eye movements studies on schizophrenics and their parents. *Eur. Neuropsychopharmacol.* 1996; **6** (Suppl. 3): 64.
15. Moriya H. A study of eye movements in patients with chronic schizophrenia and in their relatives, using an eye-mark recorder. *Psychiatr. Neurol. Jpn.* 1979; **81**: 523–558 (in Japanese).
16. Kojima T, Matsushima E, Ohta K, Toru M *et al.* Stability of exploratory eye movements as a marker of schizophrenia: A WHO multi-center study. *Schizophr. Res.* 2001; **52**: 203–213.
17. Hagiwara M, Matstushima E, Ohkura T *et al.* The relationship between explorartory eye movements in schicophrenia and gene factor. *Psychopharmacol. Bull.* 1999; **22**: 768–773.
18. Takahashi S, Matshushima E, Kojima T *et al.* Study of the families and twins of schizophrenia. In: Kojima T, Matsushima E, Ando K (eds). *Eyes and the Mind.* Japan Scientific Societies Press, Tokyo, 2000.
19. Matsushima E, Kojima T, Ohta K *et al.* Exploratory eye movements dysfunction in patients with schizophrenia; possibility as a discriminator for schizophrenia. *J. Psychiatr. Res.* 1998; **32**: 289–295.
20. Sato M, Numachi Y, Hamamura T. Relapse of paranoid psychotic state in methamphetamine model of schizophrenia. *Schizophr. Bull.* 1992; **18**: 115–122.
21. First MB, Spitzer RL, Gibbon M, Williams JBW. *Structured Clinical Interview for DSM-IV Axis I Disorders.* Biometrics Research Department, New York State Psychiatric Institute, New York, 1995.
22. Kojima T, Matsushima E, Ando K *et al.* Exploratory eye movements and neuropsychological tests in schizophrenic patients. *Schizophr. Bull.* 1992; **18**: 85–94.
23. Tandon R, DeQuardo JR, Goodson J *et al.* Effect of anticholinergics on positive and negative symptoms in schizophrenia. *Psychopharmacol. Bull.* 1992; **28**: 297–302.
24. Bell DS. Comparison of amphetamine psychosis and schizophrenia. *Br. J. Psychiatry* 1965; **111**: 701–707.
25. Ellinwood EH, Sudilovsky A, Nelson LM. Evolving behavior in the clinical and experimental amphetamine (model) psychosis. *Am. J. Psychiatry* 1973; **130**: 1088–1093.
26. Kojima T, Matsushima E, Iwama H *et al.* Visual perception process in amphetamine psychosis and schizophrenia. *Psychopharmacol. Bull.* 1986; **22**: 768–773.
27. Robinson TE, Becker JP. Behavioral sensitization is accompanied by enhancement in amphetamine-stimulated dopamine release from striatal tissue in vivo. *Eur. J. Pharmacol.* 1982; **85**: 253–254.
28. Laruelle M, Abi-Dargham A, Gil R *et al.* Increased dopamine transmission in schizophrenia: Relationship to illness phase. *Biol. Psychiatry* 1999; **46**: 56–72.
29. Sato M. Clinical and basic features of methamphetamine psychosis. *Psychiatr. Neurol. Jpn.* 2002; **104**: 179–209 (in Japanese).

Article

Low Dopamine D_2 Receptor Binding in Subregions of the Thalamus in Schizophrenia

Fumihiko Yasuno, M.D., Ph.D.
Tetsuya Suhara, M.D., Ph.D.
Yoshiro Okubo, M.D., Ph.D.
Yasuhiko Sudo, M.D., Ph.D.
Makoto Inoue, M.D., Ph.D.
Tetsuya Ichimiya, M.D., Ph.D.
Akihiro Takano, M.D., Ph.D.
Kazuhiko Nakayama, M.D., Ph.D.
Christer Halldin, Ph.D.
Lars Farde, M.D., Ph.D.

Objective: Several structural and functional brain imaging studies have pointed to a disturbance of thalamic subnuclei in patients with schizophrenia. The dopamine hypothesis of schizophrenia has, however, not been thoroughly examined in terms of this complex structure, which has connections with most brain regions of central interest in schizophrenia research. The aim of the present study was to examine dopamine D_2 receptor binding in subregions of the thalamus in patients with schizophrenia.

Method: The authors used positron emission tomography and the radioligand [^{11}C]FLB457 to examine dopamine D_2 receptor binding in thalamic subregions of 10 drug-naive patients with schizophrenia. Binding potential was calculated by the reference tissue method and used as an index for dopamine D_2 receptor binding. Comparisons were made with 19 healthy subjects. Subregions of interest were defined on individual magnetic resonance images using a percentage-based operational approach. Clinical symptoms were rated by using the Brief Psychiatric Rating Scale (BPRS).

Results: The [^{11}C]FLB457 binding potential was lower in the central medial and posterior subregions of the thalamus in patients with schizophrenia. At a functional level, there was a significant negative correlation between binding potential and BPRS positive symptom scores.

Conclusions: The subregions with low D_2 receptor binding comprise primarily the dorsomedial nucleus and pulvinar, two important components in circuitries previously suggested in the pathophysiology of schizophrenia. Aberrant dopaminergic neurotransmission in thalamic subregions might be a mechanism underlying positive symptoms in schizophrenia.

(Am J Psychiatry 2004; 161:1016–1022)

The dopamine D_2 receptor has long been of central interest in research on the pathophysiology of schizophrenia. Early positron emission tomography (PET) studies focused on the striatum, a region with a high density of D_2 receptors. Improvements in PET methodology now allow the examination of low-density dopamine D_2 receptor populations in several limbic and cortical regions in which structural or biochemical abnormalities have been reported in schizophrenia. In a recent analysis of cortical and subcortical regions, we found low radioligand binding to dopamine D_2 receptors in the anterior cingulate cortex of patients with schizophrenia and a correlation with positive symptom scores (1).

On the other hand, functional abnormality of schizophrenia has also been discussed in terms of thalamic circuitry (2). Imaging studies have consistently revealed smaller thalamic volumes in patients with schizophrenia as well as altered thalamic perfusion and metabolism (2–13). Neuropathological studies have found a reduction in the number of neurons in the mediodorsal nucleus of the thalamus in schizophrenia brains (14–17). Schizophrenia-associated neuronal loss has also been found in the pulvinar (17). A synapse-related protein study reported that the thalamic abnormalities include synaptic disturbances (18).

The thalamus was not included in early maps showing dopaminergic innervation in the rodent brain (19). However, dopamine D_2 receptors have more recently been identified in the human thalamus in vitro (20, 21) and in vivo using PET (22–24). The possibility that dopamine D_2 receptors in the thalamus are involved in the therapeutic actions of antipsychotics has been supported by PET studies that demonstrated dopamine D_2 receptor occupancy in the thalamus by antipsychotic drugs (25). Each of the major 23 subnuclei of the thalamus (26) has a unique set of efferent and afferent projections with different functional implications. In a previous study, we found a tendency toward low density of dopamine D_2 receptors in the thalamus (1). However, in that study we focused on the thalamus as a whole and did not take its detailed complexity into account.

The aim of the present PET study was to examine separately dopamine D_2 receptor binding in five major subregions of the thalamus. Ten neuroleptic-naive patients with schizophrenia and 19 healthy comparison subjects were examined with the radioligand [^{11}C]FLB457, a substituted benzamide with a very high affinity for dopamine D_2 re-